Behavior of Sliding Rubber Bearings under Horizontal Bidirectional Loadings

M. Yamamoto, S. Minewaki & N. Kamoshita
Research and Development Institute, Takenaka Corporation, Chiba, Japan

M. Kikuchi & K. Ishii
Hokkaido University, Hokkaido, Japan

O. Kouchiyama & T. Nakamura
OILES Corporation, Tochigi, Japan

SUMMARY:
A series of bidirectional loading tests were conducted on high friction type sliding rubber bearings. The sliding part of the bearing consists of a flat stainless sliding plate and a PTFE (polytetrafluoroethylene) slider of 187.5 mm diameter. The nominal friction coefficient of this bearing is 0.13. The horizontal loading path was of elliptical shape. The ellipticity was selected as a test parameter and set to 0.0, 0.25, 0.50 and 1.0. The compressive stress was 12 MPa. The force-displacement response of the sliding rubber bearing was measured. Additionally, the deformation of the rubber part was measured including the twist deformation. The maximum shear strain under bidirectional loading was as much as 1.3 times of that under unidirectional loading. A simulation analysis was also conducted on these devices and accurately represented their force-displacement relationships.

Keywords: bidirectional loading, seismic isolator, sliding rubber bearing, loading test, twist deformation

1. INTRODUCTION

In Japan, about 2,600 seismically isolated buildings and about 3,800 detached houses were constructed by 2009. During the 2011 off the Pacific coast of Tohoku Earthquake, seismic isolation systems performed well. Consequently, seismic isolation is now widely accepted in Japan.

A seismic isolation system concentrates the seismic deformation of a structure into the isolation devices. Thus, the isolation devices have a great influence on the vibration behavior of the structure. Buildings in Japan are usually designed in each horizontal direction. Similarly, seismic isolation devices have been tested and regulated in one horizontal direction. However, Yamamoto et al. (2009a, b) reported that the restoring force characteristics of high damping rubber bearings under bidirectional loadings were significantly different from those obtained under unidirectional loadings. In addition, they expressed that bidirectional loadings caused torsional deformation that increased local shear strains in the rubber bearing. The behavior of isolation devices under bidirectional loadings has to be examined for secure seismic performance of buildings.

Since the publication of the above mentioned report, bidirectional loading tests were conducted for many types of bearings. Kato et al. (2010) and Kikuchi et al. (2010) conducted bidirectional loading tests on high damping rubber bearings and lead rubber bearings, respectively.

Sliding rubber bearings which consist of a combination in series of a rubber bearing and a slider bearing have commonly been used in Japan, because they enable the period of a structure to be lengthened more easily than elastomeric isolation bearings. However, few experiments have been conducted on such bearing to observe their bidirectional behavior. This paper focuses on the mechanical properties of sliding rubber bearings especially on their horizontal bidirectional behavior. Results of such tests conducted on a series of high friction type bearing are presented.

Especially, the additional shear strains by twist deformation of the rubber part caused by bidirectional loadings were investigated. Analytical simulations of force-displacement relationships are also presented.

2. OUTLINE OF TESTS

2.1. Test specimen

Fig. 2.1 shows the test specimen. It is a scaled model of a typical sliding rubber bearing representative of those often used in Japan. The sliding part of the bearing consists of a flat stainless sliding plate and a PTFE (polytetrafluoroethylene) slider of 187.5 mm diameter. The nominal friction coefficient of this bearing is 0.13. The rubber part of the bearing is a multi-layer rubber bearing with a diameter of 225 mm, and a total rubber thickness of 11.4 mm. The shear modulus of the rubber is 0.8 MPa. This specimen has a high friction coefficient and low shear stiffness. These specifications were selected based on the commercial products of OILES Corporation which were thought to maximize the twist deformation.

One rubber part and four pairs of sliding parts were manufactured as test specimens. The same rubber part was used through the tests, whereas the sliding part was replaced after every loading pattern.
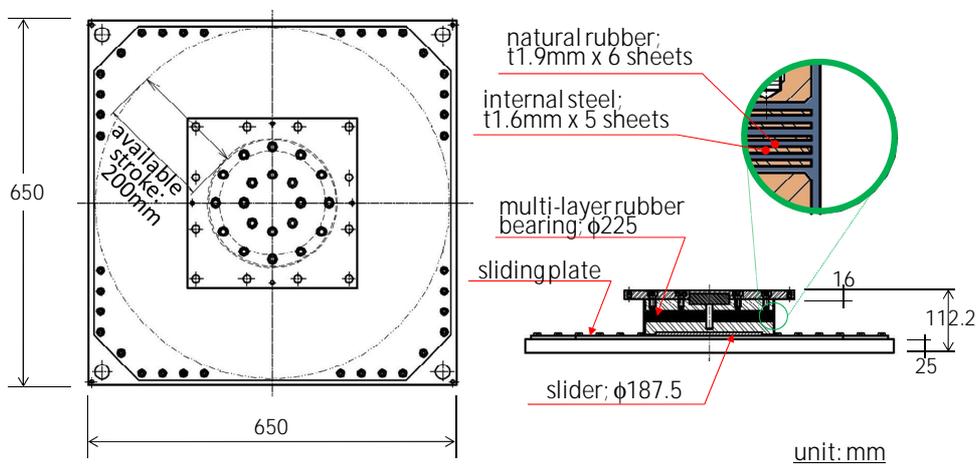

**Figure 2.1.** Test specimen

2.2. Testing system

A testing system was newly designed so that horizontal bidirectional load can be precisely applied to a test specimen with compressive vertical load to meet the research objectives. Fig. 2.2 shows the photo of the testing system. The capacities of the testing system are summarized in Table 2.1. The test specimen was set between the upper loading table that moves only in Y direction and the lower loading table that moves only in X direction. In this test, the sliding plate was set on the upper table and the rubber part with slider was set on the lower table.

Restoring forces were measured at the lower table with six degrees of freedom. They were also measured by load cells that were installed on the actuators. However, the values measured at the table were used in this paper because they were not affected by friction force of the testing machine.

Table 2.1. Capacities of Testing Machine

| Vertical force (kN)	Horizontal force (kN)		Horizontal displacement (mm)		Horizontal velocity (mm/s)	
	X	Y	X	Y	X	Y
500	200	100	+/-250	+/-250	300	300

X, main direction; Y, sub direction.
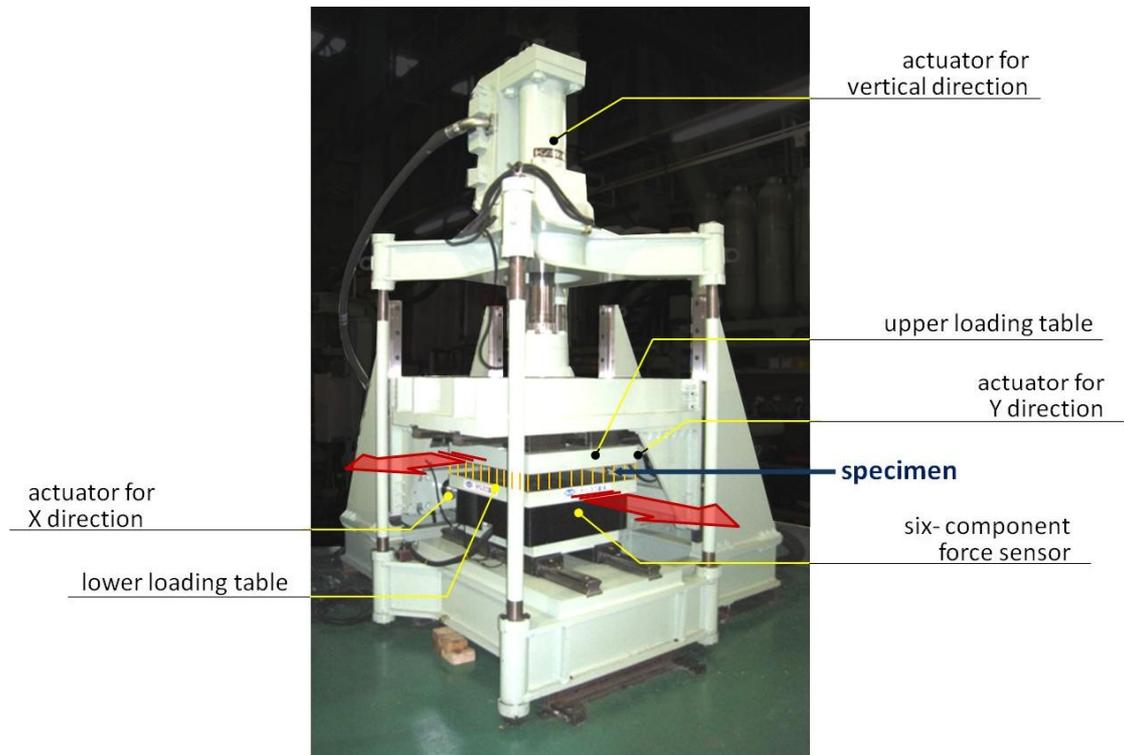
Figure 2.2. Testing system

2.3. Measurement

Actuators' displacements, actuators' forces and six force components measured at the lower table were provided by the testing machine. Besides these measurements, items that are shown in Fig. 2.3 were implemented. Potentiometer-type displacement transducers were installed to measure the deformation of rubber part directly. By using four displacement transducers, twist deformation as well as two horizontal deformations were obtained.
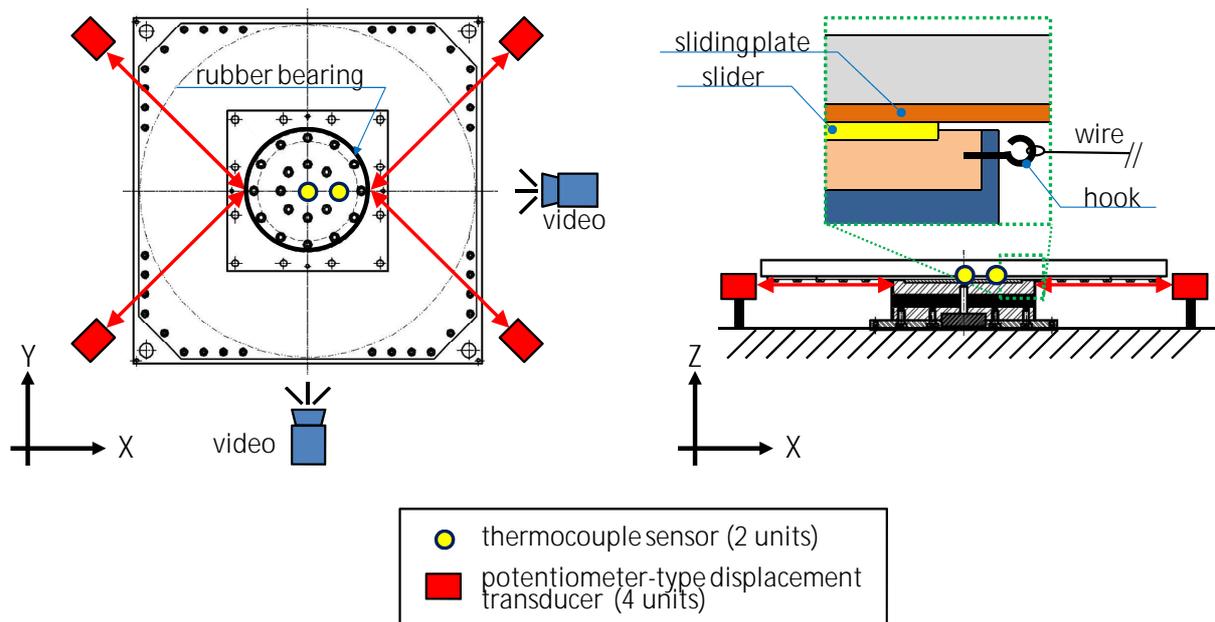
**Figure 2.3.** Measuring equipment

2.4. Loading pattern

A loading orbit can be expressed in two horizontal orthogonal directions as a pair of sinusoidal waves with same amplitude, A_0, and a phase shift, θ.

$$\begin{cases} X_0 = A_0 \sin(\phi) \\ Y_0 = A_0 \sin(\phi + \theta) \end{cases} \tag{2.1}$$

where X_0 and Y_0 are orthogonal horizontal axes, and ϕ is the phase of the movement. By changing the phase shift, θ, Eq. 2.1 can produce any elliptical shape from a straight line to a circle. Fig. 2.4 shows orbits that are obtained from Eq. 2.1 with $\theta = 0°, 28°, 53°$ and $90°$. X and Y in Fig. 2.4 are the main and sub loading axes that rotate 45 degree with respect to X_0 and Y_0. Ellipticities of these ellipses are 0, 0.25, 0.5 and 1.0. These four loading patterns were used in the tests.

The loading paths start from the origin to $+Y_0$ direction first. After complete three and quarter loops, they return to the origin toward $-X_0$ direction.

The parameter A (= $\sqrt{2} \times A_0$) that is the amplitude of a unidirectional loading was introduced. Four levels, A = 50, 100, 150, 200 mm, were used in the tests. The loading speed of 30 mm/s was kept constant for all loading cases.
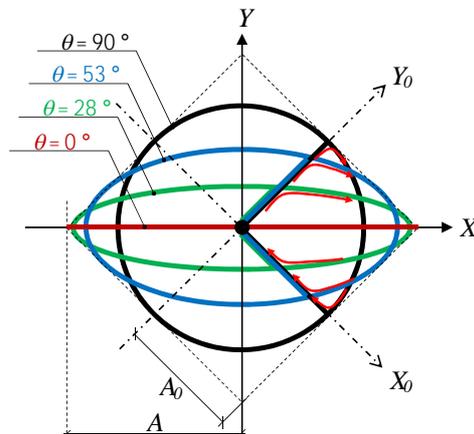

Figure 2.4. Displacement orbits by phase shift

3. TEST RESULTS

3.1. Restoring force

Force-displacement relationships are plotted in Fig. 3.1 for the loading case of maximum amplitude, A = 200 mm, and each phase shift, θ. Plots (a) and (d) show the force-displacement relationships of the sliding rubber bearing as a whole. Plots (b) and (e) show the force-displacement relationships of the rubber part only. Plots (c) and (f) show force-displacement relationships of the slider part only.

The hysteresis loops exhibit round shape due to bidirectional loading. This tendency was dominant for large value of θ. If the rubber part was linear elastic, plots (b) and (e) for bidirectional loading would show the same relationship for any value of θ. Although the rubber part was made of natural rubber, it showed hardening and relative large damping characteristics under unidirectional loading as shown in plot (b) of Fig. 3.1.(i). Then, the force-displacement relationship varied depending on the value of θ. The temperature started at 20 °C and ended about 50 °C at the highest.
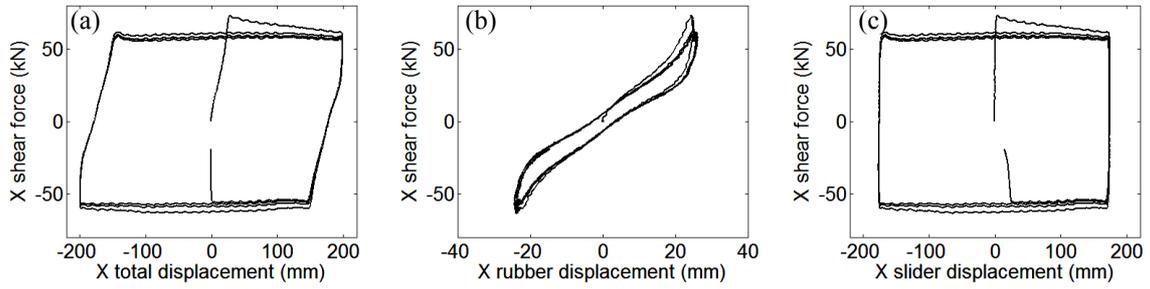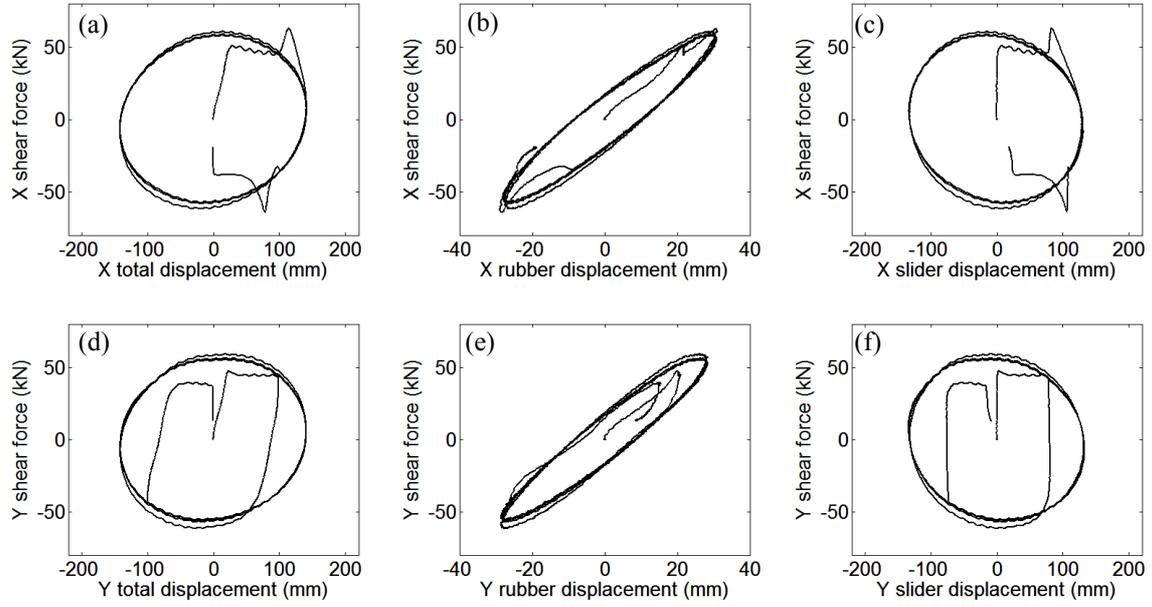
(i) $\theta = 0°$; unidirectional loading
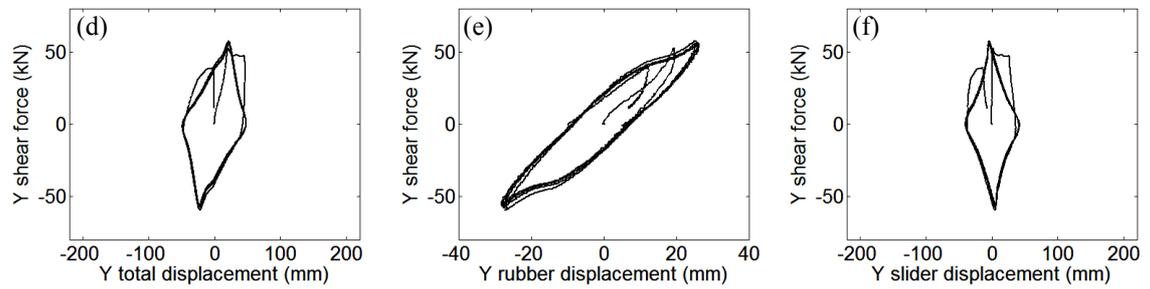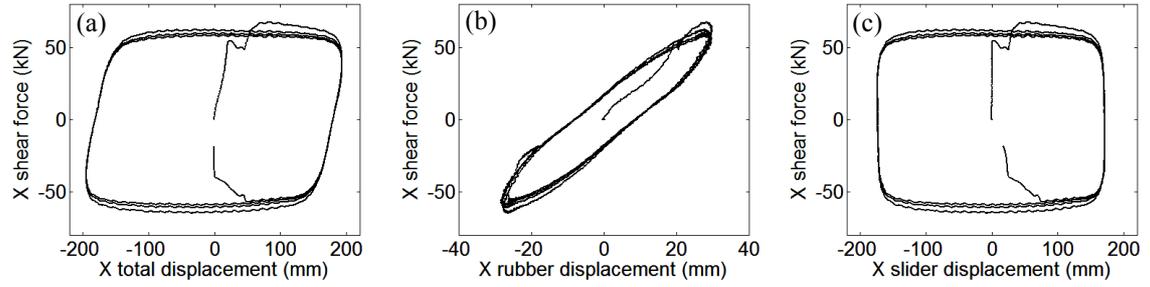
(ii) $\theta = 28°$; ellipticity, 0.25
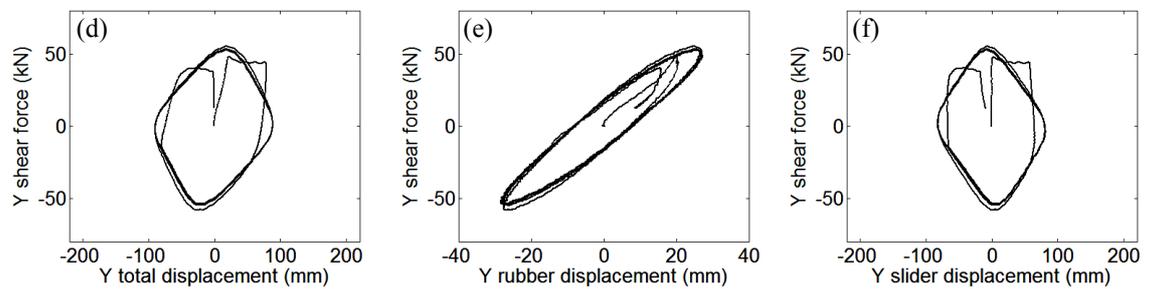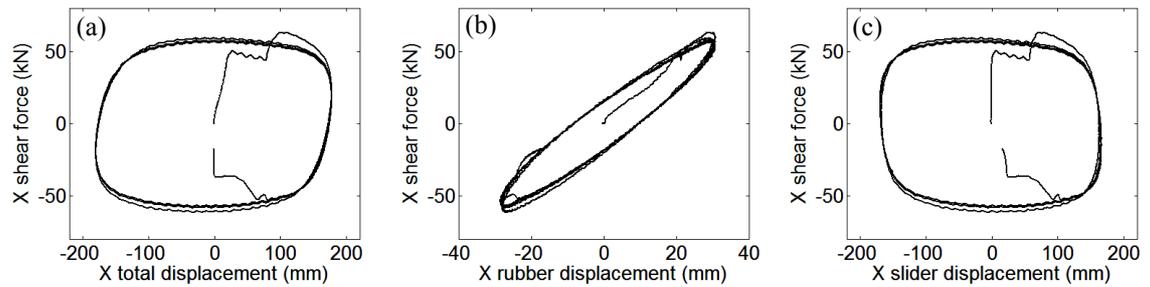
(iii) $\theta = 53°$; ellipticity, 0.50

Figure 3.1. Force-displacement relationships

(iv) $\theta = 90°$; circle loading

Figure 3.1.(continued) Force-displacement relationships

3.2. Deformation of rubber

Equilibrium of forces that acted on the rubber part was assumed as shown in Fig. 3.2. Where (D_x, D_y) and (F_x, F_y) represent horizontal deformations and horizontal restoring forces of the rubber part, respectively. M_{z0} and M_{z1} represent the twist moment of rubber part at the lower and the upper flanges, respectively.

Based on the measured values of M_{z0}, D_x, D_y, F_x and F_y, M_{z1} can be calculated as follows.

$$M_{z1} = M_{z0} + F_x \times D_y \quad F_y \times D_x \tag{3.1}$$

The distribution of the twist moment, $M(z)$, with respect to the rubber height, z, was assumed as:

$$M(z) = M_{z0} \quad M_{z1} \quad M_{z0} \quad z \quad h \tag{3.2}$$

where h is the total height of rubber. Fig. 3.2 illustrates the twist moment distributions. The displacement at circumference of the rubber induced by the twist deformation, u, was derived as

$$u = \int_0^h \frac{M(z)}{G \times I_p} \frac{d}{2} dz \tag{3.3}$$

Hence,

$$Gu = \int_0^h \frac{M(z)}{I_p} \frac{d}{2} dz = \frac{d}{2} \left(\frac{M_{z1} + M_{z0}}{2I_p} \right) h \tag{3.4}$$

where I_p, G and d are the polar modulus of the section, shear modulus and diameter of the rubber part. The relation between u and the right-hand side of Eq. 3.4 was plotted in Fig. 3.3 considering $I_p = 2.51 \times 10^8$ mm⁴, $d = 225$ mm and $h = 11.4$ mm. The gradient of Fig. 3.3 corresponds to an effective shear modulus for twist deformation. The shear modulus was roughly evaluated as $G = 1.0$ N/mm².
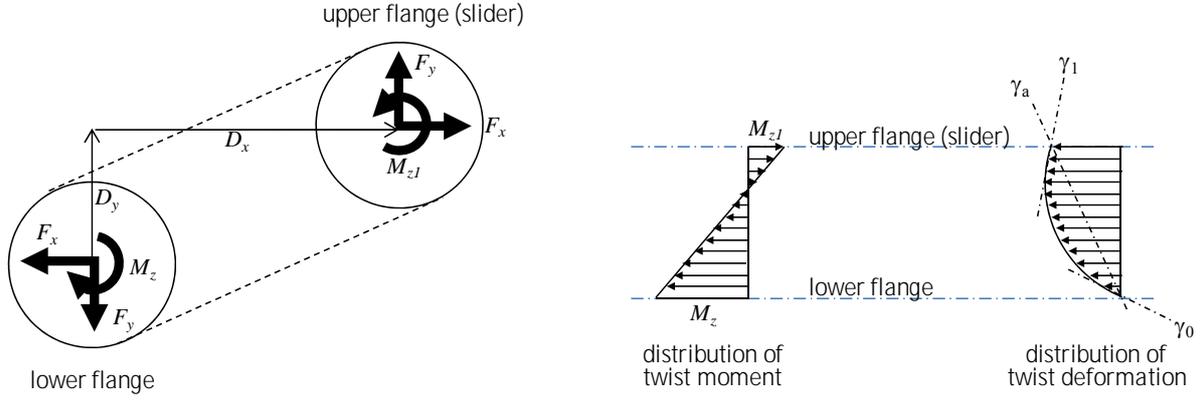
Figure 3.2. Equilibrium of forces and assumed distribution of twist deformation
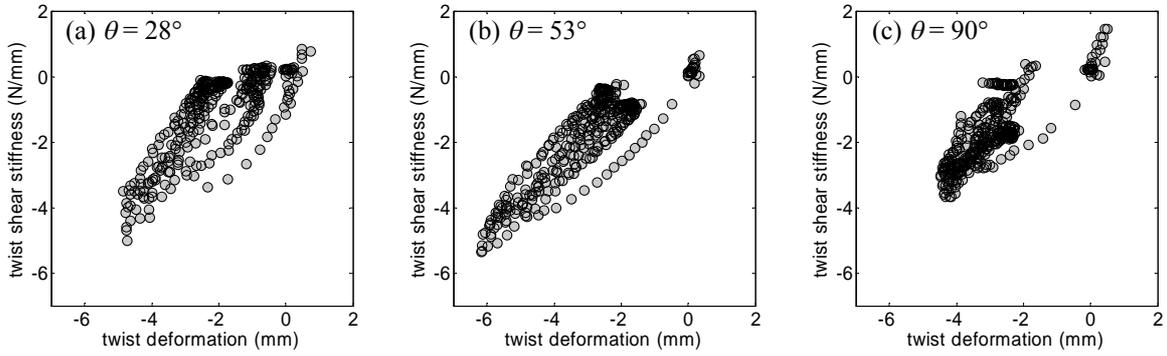
**Figure 3.3.** Relation between twist deformation and twist shear stiffness

The additional shear strains by the twist deformation varied according to the vertical position within the rubber. The distribution of the additional shear strain was assumed as shown in Fig. 3.2. γ_0 and γ_1 are the additional shear strains at both the lower and upper flanges. They are calculated as:

$$\gamma_0 = \frac{d}{2}\frac{1}{GI_p}M_{z0}h = \gamma_a - \frac{d}{2}\frac{1}{GI_p}\left(\frac{M_{z1}-M_{z0}}{2}\right)h = \gamma_a - \frac{d}{2}\frac{1}{GI_p}\left(\frac{F_xD_y-F_yD_x}{2}\right)h \qquad (3.5)$$

$$\gamma_1 = \frac{d}{2}\frac{1}{GI_p}M_{z1}h = \gamma_a + \frac{d}{2}\frac{1}{GI_p}\left(\frac{M_{z1}-M_{z0}}{2}\right)h = \gamma_a + \frac{d}{2}\frac{1}{GI_p}\left(\frac{F_xD_y-F_yD_x}{2}\right)h \qquad (3.6)$$

where γ_a (= u/h) is the average additional shear strain. The additional shear strains for the case of $A =$ 200 mm were plotted in Fig. 3.4, where γ_a was obtained from displacement measurements, and γ_0 and γ_1 were calculated from Eqs. 3.5 and 3.6, respectively, by assuming $G = 1.0$ N/mm^2. Fig. 3.5 shows the average shear strain, additional shear strain at the lower flange, γ_0, and maximum shear strain. The average shear strain is the total horizontal deformation of rubber part at the center of slider divided by the total rubber thickness. The maximum shear strain is the sum of the average shear strain and maximum additional shear strain γ_0. Table 3.1 shows the maximum values of shear strains for each value of θ. Fig. 3.6 (ii) shows the deformation of the rubber when the center of the slider was right on the X-axis. The twist deformation of the rubber can clearly be observed on this figure.

It was found that 1) twist deformation was observed even under unidirectional loading, 2) average shear strain increased because the equivalent shear stiffness was reduced (see Fig. 3.1) by bidirectional loading, 3) additional shear strain reached 66% at the circumference of the rubber part, however, the increased value of maximum shear strain from average shear strain was about 42% because they did not reach their maxima at the same time.
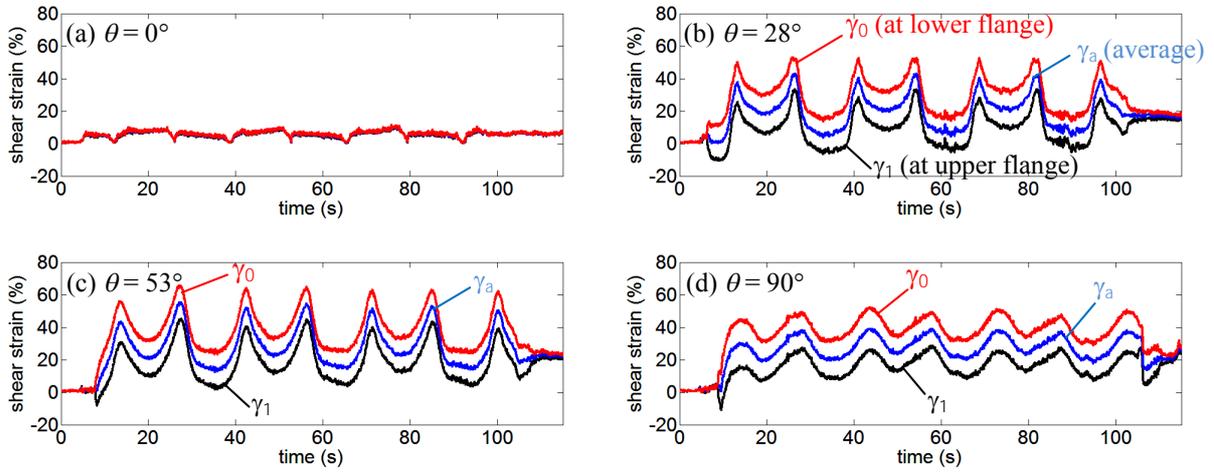
Figure 3.4. Additional shear strains caused by twist deformation for the case of $A = 200$ mm
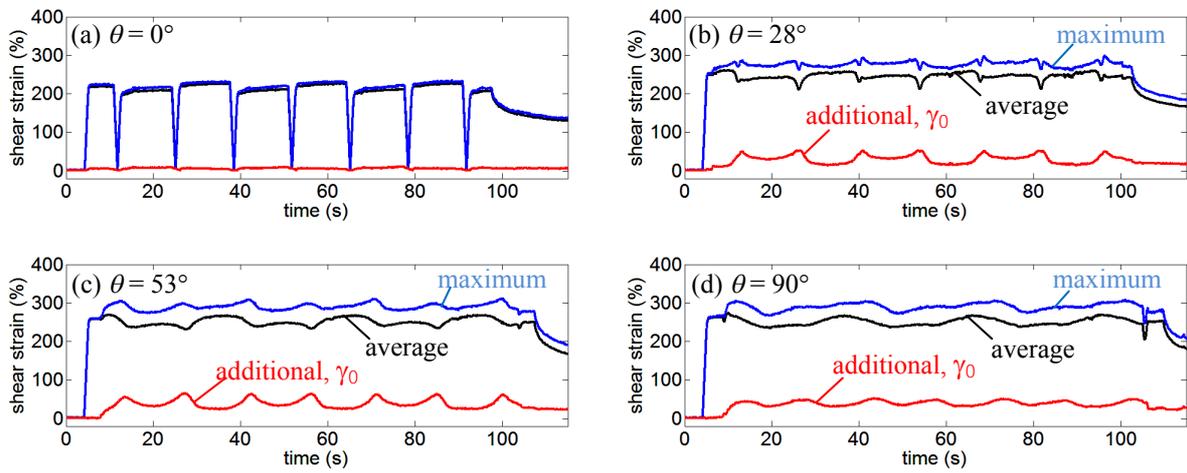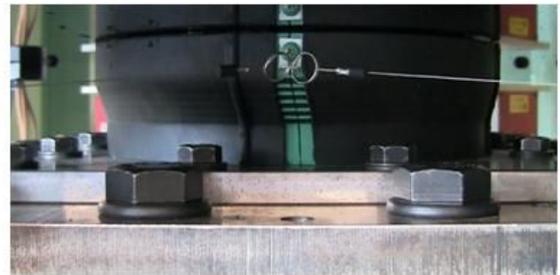

Figure 3.5. Comparison of shear strains

Table 3.1. Maximum Values of Shear Strains

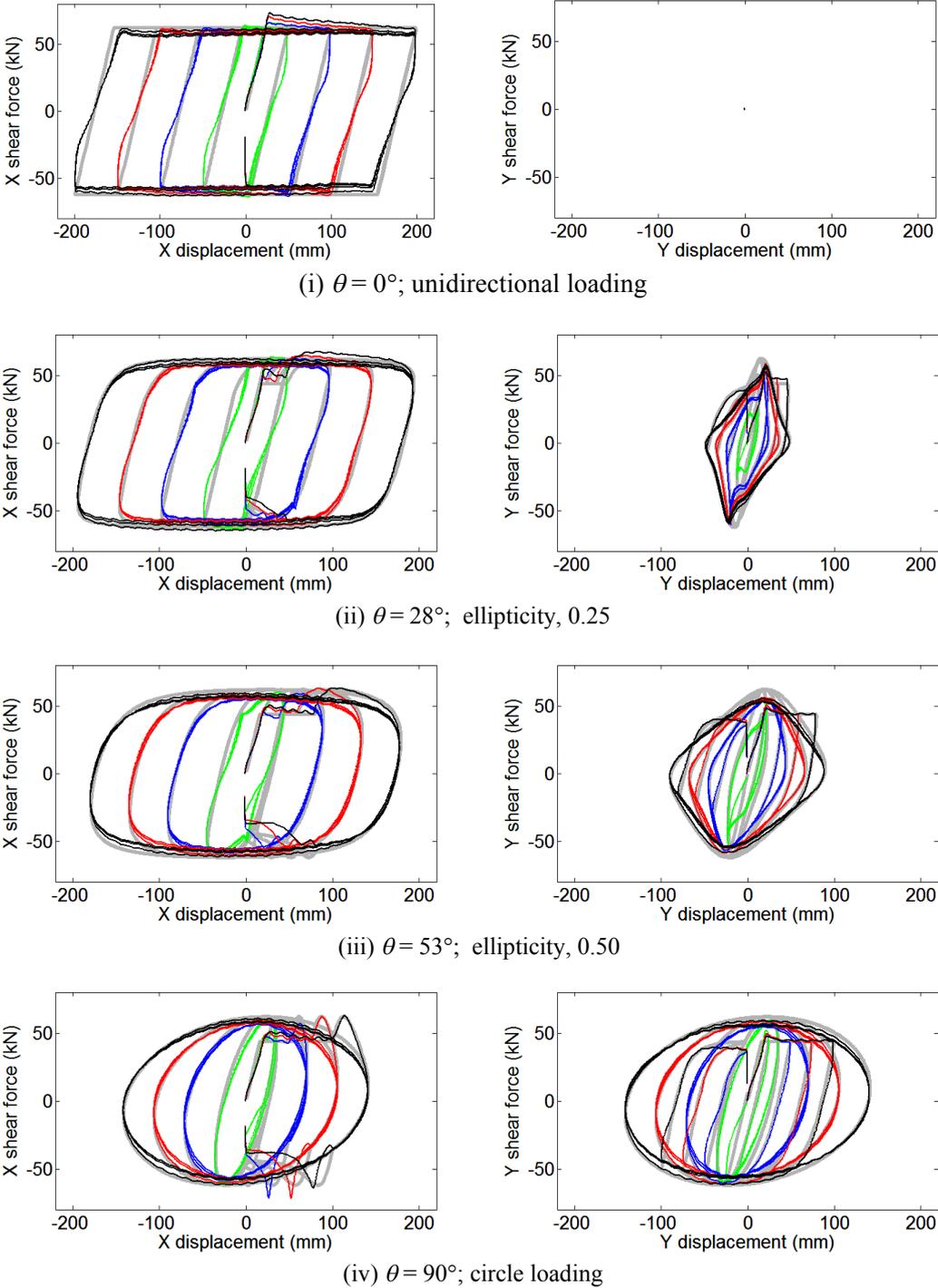|		Unidirectional loading, $\theta = 0°$.	Bidirectional loading		
			$\theta = 28°$	$\theta = 53°$	$\theta = 90°$
Average shear strain (%)		229	261	270	274
Additional shear strain by twist deformation (%)	at upper flange, γ_1	11	34	45	30
	at lower flange, γ_0	12	53	66	52
	average, γ_a	11	43	55	39
Maximum shear strain (%)		236	299	312	308

(i) unidirectional loading

(ii) bidirectional loading ($\theta = 53°$)
(twist deformation was observed)

Figure 3.6. Side view of the rubber part when the center of slider was right on the X-axis;
cover rubber was peeled to observe the rubber deformation

4. ANALYTICAL SIMULATION

The force-deformation relationships were simulated using a perfect elasto-plastic model defined in two horizontal directions. The friction coefficient was constant and set as 0.13 for all the loading cases. Fig. 4.1 shows the analytical and experimental hysteresis loops. Except for the elastic characteristics especially observed in Fig. 4.1.(i) that was caused by hardening of the rubber part, this simple analytical model was able to predict the test results accurately for all the loading cases.

(i) $\theta = 0°$; unidirectional loading

(ii) $\theta = 28°$; ellipticity, 0.25

(iii) $\theta = 53°$; ellipticity, 0.50

(iv) $\theta = 90°$; circle loading

Figure 4.1. Comparison of analytical and experimental hysteresis loops; thick gray lines show analytical results; green, blue, red and black lines show experimental results for $A = 50, 100, 150$ and 200 mm, respectively

5. CONCLUSION

A series of bidirectional loading tests were conducted on a typical sliding rubber bearing often used in Japan. The specimen was a scaled model selected from the commercial products by OILES Corporation to enhance the twist deformation. After the tests, neither damage nor deterioration characteristics were observed. Bidirectional loadings in this test series did not affect the device itself. However, it is important to design this type of bearing considering the findings presented in this paper.

By bidirectional loading, the rubber part experienced twist deformation. This deformation corresponded to the shear strain of 66% at circumference of rubber part, which was not negligible. Furthermore, the equivalent stiffness was reduced by bidirectional loading, inducing an increase in the average shear strain. Because of these effects, the shear strain under bidirectional loading was increased as much as 1.3 times of that under unidirectional loading.

The importance of vertical pressure should be pointed out. By increasing the vertical pressure, both the shear force and shear deformation will increase. The twist moment depends on the product of these values. Then, the effect of twist deformation approximately increases with the square of the vertical pressure.

Simulation analyses were also conducted using a perfect elasto-plastic model defined in two horizontal directions. This simple analytical model was able to predict accurately the test results for all the tested cases.

REFERENCES

Kikuchi M., Aiken I. D. (1997). An analytical hysteresis model for elastomeric seismic isolation bearings. *Earthquake Engineering & Structural Dynamics*, **26**, 215–231.

Minewaki S., Yamamoto M., Higashino M., Hamaguchi H., Kyuke H., Sone T., Yoneda H. (2009). Performance tests of full size isolators for super high-rise isolated buildings. *J. of Structural Engineering, AIJ*, **55B**, 469-477 (in Japanese).

Yamamoto M., Minewaki S., Yoneda H., Higashino M., Wada A. (2009a). Full-scale tests and analytical modeling of high-damping rubber bearings under two horizontal directional loading. *J. of Struct. Constr. Eng, AIJ*, **74**, 639-645 (in Japanese).

Yamamoto M., Minewaki S., Higashino M., Hamaguchi H., Kyuke H., Sone T., Yoneda H. (2009b). Performance tests of full size rubber bearings for isolated superhigh-rise buildings. *International Symposium on Seismic Response Controlled Buildings for Sustainable Society, Tokyo, Japan*, SI-4.

Kato H., Shimooki W., Murota N., Kitamuara H., Yamamoto M. (2010). An experimental study on physical properties of high-damping rubber bearings under biaxial loading. *Summaries of Tech. Papers of Annual Meeting, AIJ*, **B2**, 261-264 (in Japanese).

Kikuchi M., Nakamura T., Ishii K., Suzuki Y. (2011). Mechanical properties of lead rubber bearings under biaxial loading. *Summaries of Tech. Papers of Annual Meeting, AIJ*, **B2**, 505-508 (in Japanese).

Yamamoto M., Kikuchi M., Ishii K., Yoneda H., Minewaki S., Kato H. (2011). Bi-axial horizontal response for a seismically-isolated building with high-damping rubber bearing, *12th World Conference on Seismic Isolation, Sochi, Russia*.

Yamamoto M., Minewaki S., Yoneda H., Higashino M. (2012). Nonlinear behavior of high-damping rubber bearings under horizontal bidirectional loading: full-scale tests and analytical modeling. *Earthquake Engineering & Structural Dynamics*, DOI: 10.1002/eqe.2161.